

# Topology-Scaling Identification of Layered Solids and Stable Exfoliated 2D Materials

Michael Ashton,<sup>1</sup> Joshua Paul,<sup>1</sup> Susan B. Sinnott,<sup>2</sup> and Richard G. Hennig<sup>1</sup>

<sup>1</sup> Department of Materials Science and Engineering,  
University of Florida, Gainesville, FL 32611-6400

<sup>2</sup> Department of Materials Science and Engineering,  
The Pennsylvania State University, University Park, PA 16801-7003

(Dated: March 6, 2024)

The Materials Project crystal structure database has been searched for materials possessing layered motifs in their crystal structures using a topology-scaling algorithm. The algorithm identifies and measures the sizes of bonded atomic clusters in a structure's unit cell, and determines their scaling with cell size. The search yielded 826 stable layered materials that are considered as candidates for the formation of two-dimensional monolayers via exfoliation. Density-functional theory was used to calculate the exfoliation energy of each material and 680 monolayers emerge with exfoliation energies below those of already-existent two-dimensional materials. The crystal structures of these two-dimensional materials provide templates for future theoretical searches of stable two-dimensional materials. The optimized structures and other calculated data for all 826 monolayers are provided at <https://materialsweb.org>.

The combination of modern computational tools and the growing number of available crystal structure databases with high-throughput interfaces have accelerated recent efforts to map the materials genome. One of the most recently discovered branches of the materials genome is the class of two-dimensional (2D) materials, which generally have properties that are markedly different from their three-dimensional counterparts. The canonical example is the graphite/graphene system, but monolayers have been exfoliated from many other layered compounds as well [1–4]. Stable 2D materials can also be obtained by deposition [5–8] or chemical exfoliation [9, 10]. Because the contribution of interlayer interactions to these materials free energies is typically quite small, the existence of a mechanically exfoliable bulk precursor generally indicates the relative stability of a free-standing single layer, regardless of how it is synthesized.

In an effort to discover novel 2D materials, two recent studies searched the inorganic crystal structure database (ICSD) for compounds with large interlayer spacings, which are characteristic of weak interlayer bonding that could be overcome by mechanical exfoliation [11, 12]. They used the intuitive criteria of a low packing fraction based on the covalent radii of the atoms and an interlayer gap larger than the sum of the covalent radii of atoms at the layers' surfaces along the  $c$ -axis to identify layered compounds in the ICSD. They discovered almost 100 layered phases, nearly half of which had monolayers that had not been the subject of any prior publications.

Here, we extend their method to identify a large number of layered compounds that were missed using the packing factor and  $c$ -axis interlayer gap criteria. We further add the constraint that a bulk material must be thermodynamically stable to be of interest during our search. Therefore, we use the Materials Project (MP) database [13], an online repository of crystallographic and thermodynamic data for over 65,000 compounds calculated with

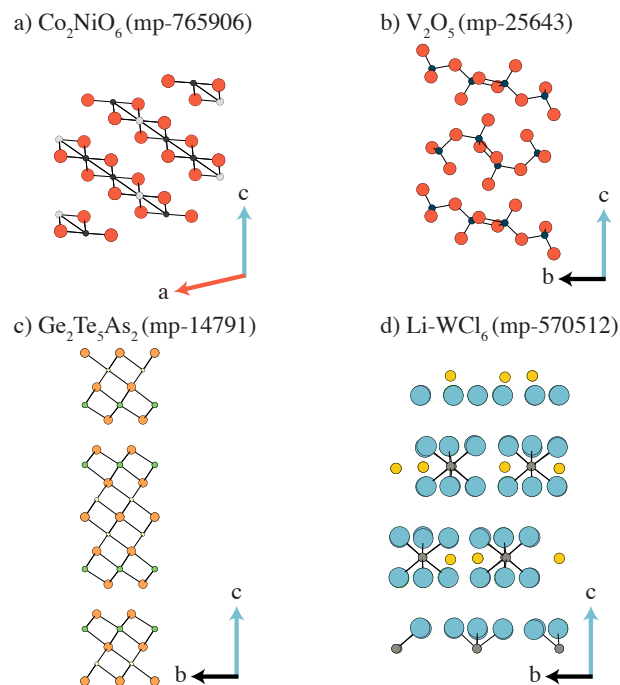


FIG. 1: (Color online) Examples of structure types that challenge the search for layered materials by exhibiting a) layers along an axis other than the  $c$ -axis, b) corrugated layers, c) thick layers, and d) molecular (non-bonded) layers. Each of these examples is correctly classified with the present method.

density-functional theory (DFT).

Our algorithm is designed to correctly identify additional layered materials by handling four different cases that are illustrated in Fig. 1: (a) materials whose layers are not perpendicular to unit-cell axes or parallel to unit cell surfaces, (b) materials with corrugated layers that therefore lack a planar interlayer spacing, (c) materials with very thick layers that exceed the packing factor normally observed for layered materials, and (d) materi-

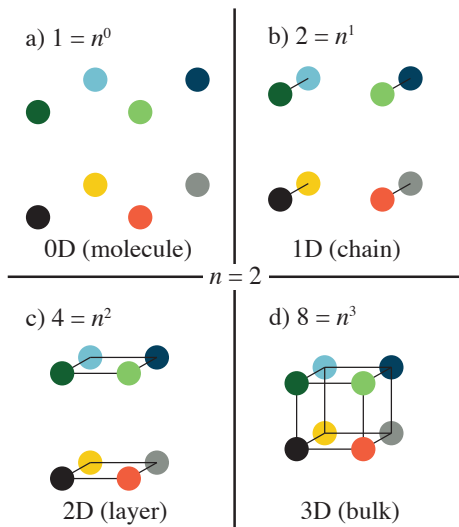


FIG. 2: (Color online) Schematic of the topology-scaling algorithm (TSA). The black circle (bottom left in each frame) represents a cluster of bonded atoms in a given crystal structure’s unit cell. The colored circles represent the seven periodic images of the same cluster for a  $2 \times 2 \times 2$  supercell of the original cell. The periodic images are either bonded to one another in a) zero, b) one, c) two, or d) three dimensions, defining the dimensionality of the structural motifs.

als composed of molecular species that have gaps along multiple axes and are often identified as false positives.

Each of these cases is correctly classified using our topology-scaling algorithm (TSA) to identify layered compounds. The first step in the TSA is to isolate bonded clusters of atoms in the structure, where a bond is defined as an overlap in the covalent radii of two neighboring atoms plus a small tolerance. If all atoms in the structure are in the same cluster, the structure is classified as a conventional bulk compound. If not, we count the number of atoms in a single cluster, create an  $n \times n \times n$  supercell of the original structure, and group all atoms into bonded clusters again. The scaling of the cluster size with supercell size,  $n$ , determines the dimensionality of the structure as illustrated in Fig. 2. If the number of atoms in the original cluster does not change with supercell size (zeroth order scaling), the cluster is an isolated molecule or atom. If the number of atoms scales linearly with  $n$ , the cluster is a one-dimensional chain. If it scales as  $n^2$ , it is a true layered solid. If it scales as  $n^3$ , it is most likely an intercalated solid (*e.g.* a lithiated zeolite) composed of a three-dimensional bonded network structure with intercalated atoms or molecules.

Here, we use the TSA to identify layered solids, but its ability to simultaneously identify bonded networks of any dimension is what allows it to systematically classify structures in large materials databases. Correctly distinguishing between molecular, intercalated, and layered solids is crucial, since there are large numbers of

molecular and intercalated structures in most materials databases.

The strength of the TSA is that it discovers structural motifs that are separated from each other by distances larger than the bond length of atoms within the motifs. The search for bonded clusters employs a range of bond-length tolerances between 100% and 135% of the summed covalent radii [14]. A few compounds are only identified as layered for a small range of tolerances; these are visually examined.

Our algorithm identifies 1560 layered materials, 509 of which have zero distance to their respective thermodynamic convex hulls, and hence are predicted to be stable compounds. Another 590 materials are metastable by less than 50 meV/atom, 206 by between 50 and 100 meV/atom, and 255 are unstable by more than 100 meV/atom. Here, we focus on the stable and metastable materials with distances to the hull of less than 50 meV/atom. Additionally, several of the 1560 layered materials are simply different stacking sequences of the same monolayer. These duplicates are filtered out using symmetry analysis resulting in 826 unique monolayers for further investigation.

These 826 materials can be grouped according to their stoichiometric ratios. Fig. 3(a) shows that 50% of the layered materials are represented by just five stoichiometries. These five –  $AB_2$ ,  $ABC$ ,  $AB$ ,  $AB_3$ , and  $ABC_2$ , in decreasing order of frequency – mostly reflect the abundance of known 2D materials with simple cation/anion stoichiometries. However, the large variety of 102 unique stoichiometries indicates that the family of potentially exfoliative layered compounds is much more diverse than the simple compositions typically considered as 2D material candidates.

Figure 3(b) and (c) compare the percentages of unary, binary, ternary, *etc.* stable layered compounds in the MP database with the percentages of all stable (distance to hull  $< 50$  meV/atom) compounds in the MP database. Binary, ternary, and quaternary compounds comprise 98.2% of the stable layered compounds. The percentages of unary and ternary compounds among layered materials are very close to their percentages among all materials in the MP database. However, binary compositions are clearly overrepresented among layered materials, while quaternary and quinary compositions are underrepresented. This indicates that compounds of two or three species can more easily form low-energy structures that exhibit dispersion-bound layers.

These materials can be further classified according to their crystal structures, which has implications for future searches for 2D materials based on chemical substitutions and genetic algorithms [15, 16]. The crystal structures represented by each stoichiometry can be used as templates for these searches, which require viable crystal structures as the initial parent structures to seed the algorithm. The use of a larger number

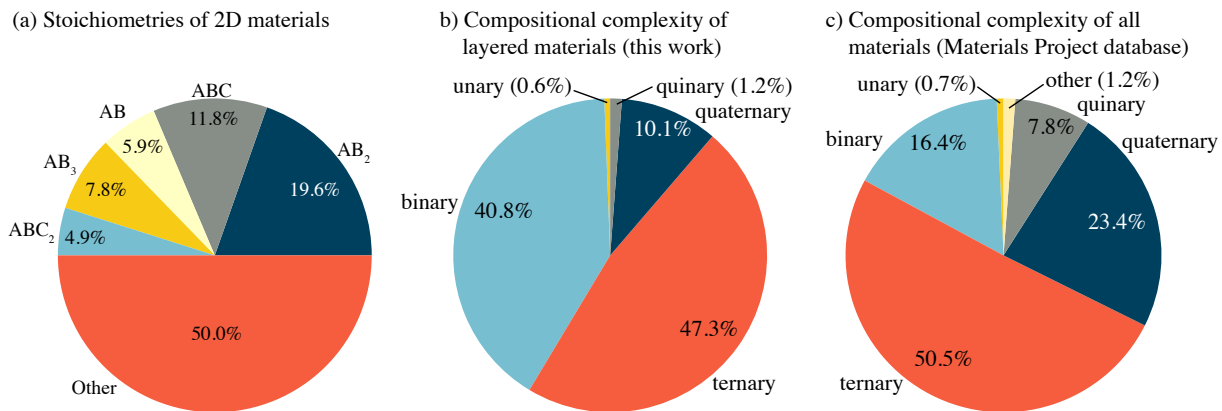


FIG. 3: (Color online) Distribution of (a) stoichiometries of the 826 layered compounds, and comparison of the compositional complexity among (b) the stable layered materials identified by this work and (c) all materials in the Materials Project database. The top 5 stoichiometries (ABC, AB<sub>2</sub>, AB, AB<sub>3</sub>, and ABC<sub>2</sub>) represent half of all compounds. In general, the relative abundance of a given stoichiometry scales inversely with the formula’s complexity. We observe that the percentage of binary compounds among layered materials is significantly higher than among all materials, suggesting that binary compounds (one cation and one anion) are particularly conducive to creating interlayer dispersion interactions.

of seed structures increases the likelihood that a given search will identify the global minimum of a composition’s high-dimensional phase space. The complete set of the structural templates for all stoichiometries identified by our algorithm is available online in our database at <https://materialsweb.org>.

An example of structural templates is given in Fig. 4, which shows all 15 unique crystal structures identified for the AB stoichiometry. These 15 structures can either augment or stand alone as the parent generation in future searches for 2D materials of AB composition. These various structures will likely possess a wide variety of properties, even for the same A and B elements. For example, buckled structures, such as structures (i) and (m) in Fig. 4, are uniquely interesting because their broken inversion symmetry could lead to piezoelectricity [17–21] or, given sufficiently large spin-orbit coupling, to Rashba spin splitting [22, 23]. For lubricating applications, flat monolayers like structures (f) and (h) may exhibit lower friction coefficients than strongly buckled monolayers, like structures (c) and (o). Top and side views of these 2D structures are provided in the Supplemental Material [24].

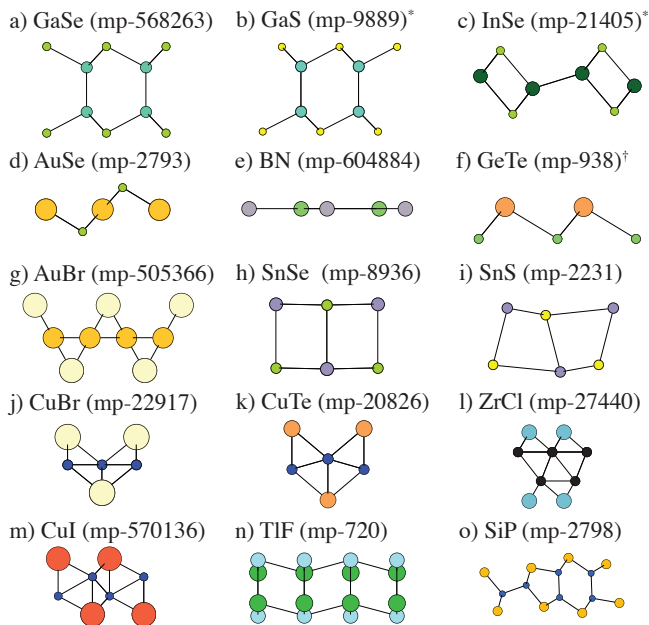
We re-optimize the structures of all 826 stable layered materials and the single monolayers from each structure with DFT using VASP [25–28]. We employ the dispersion-corrected vdW-optB88 exchange-correlation functional [29–32] to accurately account for interlayer dispersion interactions. Comparison with more accurate and computationally demanding random-phase approximation (RPA) calculations [11] show that this functional reproduces relative trends in exfoliation energy and predicts the interlayer interactions within 30% of the RPA. We compare the resulting exfoliation energy of the single monolayer materials, given by the energy difference

between the monolayer and the bulk solid, with that of free-standing monolayers that have previously been synthesized. As an upper bound, 2D SnSe has been synthesized [33, 34] and has an exfoliation energy close to 150 meV/atom. The most promising 2D material candidates will have much lower exfoliation energies, but monolayers with exfoliation energies below 150 meV/atom may be feasible for synthesis [16, 35].

Fig. 5 shows the distribution of calculated exfoliation energies for all 826 compounds with respect to the exfoliation energies of known 2D materials. A large majority of 680 compounds have exfoliation energies below 150 meV/atom, and most (612) have exfoliation energies below 100 meV/atom.

We find that C, P, As, Sb, and Bi are the only elements that have pure layered forms. Of those five, Sb and Bi share the same structure, as do P and As, leading to the three unique unary layered crystal structures shown in Fig. 6. Graphene (C), phosphorene (P), arsenene (As), and antimonene (Sb) have all been reported as 2D materials experimentally and/or theoretically [36–39], but very little work has been done to isolate or characterize bismene (Bi) nanosheets. The exfoliation energy of bismene is 273 meV/atom, similar to that of 2D Sb (236 meV/atom). Both are above the 150 meV/atom threshold of exfoliation energies for experimentally existent materials, but still much more stable than silicene [40, 41], which has been stabilized on substrates. Thus, 2D bismene, if not stable as a free-standing monolayer, may be stabilized on a suitable substrate [42, 43]. Top and side views of these 2D structures are provided in the Supplemental Material [24].

To illustrate the variety of properties accessible among the 826 2D materials we have identified, 182 are predicted to exhibit magnetic moments larger than 1  $\mu_B$ /unit cell



\* Not minimum energy structure for any compound we observed.

† Exfoliation energy over 200 meV/atom.

FIG. 4: (Color online) Side views of the 15 unique structural templates identified for monolayers of AB stoichiometry, labeled according to prototypical compounds possessing that crystal structure. The symmetries of structures a) and b) are related by a broken inversion symmetry, in the same way that the well-known 1T and 2H monolayer structures are related. Other structural pairs, such as e), f) and h), i) and j), k), are related to one another by simple buckling distortions.

and 519 display band gaps at the PBE level. Only ferromagnetic configurations were considered; more detailed analysis will be required to determine which magnetic 2D materials have antiferromagnetic or more complex orderings.  $\text{CaClF}$  and  $\text{MgCl}_2$  have the largest band gaps at the PBE level of both 6 eV. Their inexpensive constituent elements and relatively substrate-agnostic interlayer interactions make  $\text{CaClF}$  and  $\text{MgCl}_2$  particularly interesting candidates for thin transparent dielectrics in electronic device technologies.

Thirty of the magnetic 2D materials exhibit half-metallic character; that is, exactly one of their spin channels is metallic. The band structure of  $\text{FeCl}_2$ , an example half-metallic material, is provided in Figure 7. This material’s minority spin state is metallic, while its majority state is insulating with a relatively large gap of 4.4 eV. Electrical currents in 2D  $\text{FeCl}_2$  and other half-metals will in principle be completely spin-polarized [44–46], enabling the giant magnetoresistive effect that powers many spintronic devices [47]. These materials are therefore of significant technological interest, as their dispersive interlayer interactions make them uniquely adaptable to vertically stacked heterostructures in, for example, spin

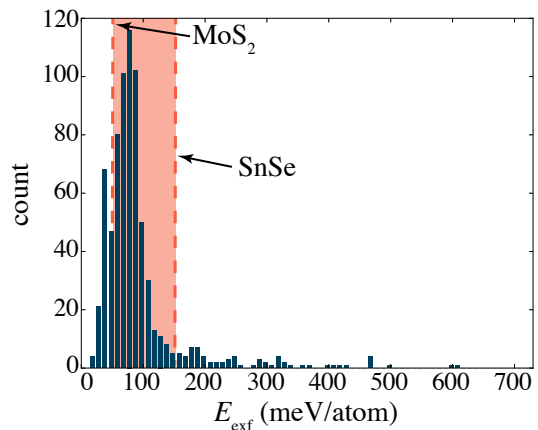


FIG. 5: (Color online) Histogram of calculated exfoliation energies for all 826 layered materials compared to the range of calculated exfoliation energies for already synthesized 2D materials. Because of their relatively weak interlayer forces, most compounds found in our search exhibit low exfoliation energies ( $< 100$  meV/atom), indicating the ease of exfoliation.

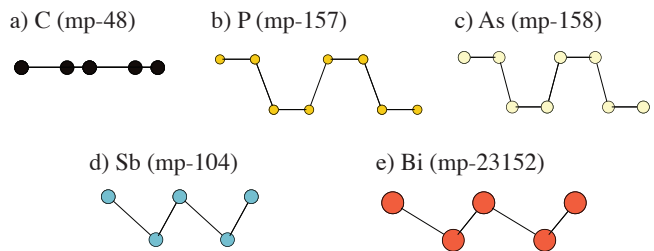


FIG. 6: Side views of monolayers for the five elemental layered materials in the Materials Project database.

valves [48, 49] and Josephson junctions [50].

To view interactive and downloadable information for all structures, including exfoliation energies, input files used for calculations, band structures, and calculated Pourbaix diagrams, the reader is again referred to our online database at <https://materialsweb.org>.

In summary, we developed a general topology-based algorithm that classifies crystal structures by the dimensionality of their structural motifs and applied it to predict the stability of more than 600 potential 2D materials, including bismene, which may be the most stable elemental 2D material left to be synthesized. The synthesis and further characterization of these materials could, in turn, unearth a commensurate wealth of materials properties. Additionally, the monolayer structures identified in this search can serve as viable structural templates for theoretical searches for 2D materials, such as genetic algorithm and chemical substitution searches, that may lead to the discovery of many more stable 2D materials.

The authors thank Dr. Vin Crespi for valuable discussions. M.A. and S.B.S. were supported by the National Science Foundation under grant DMR-1307840, and J.P.

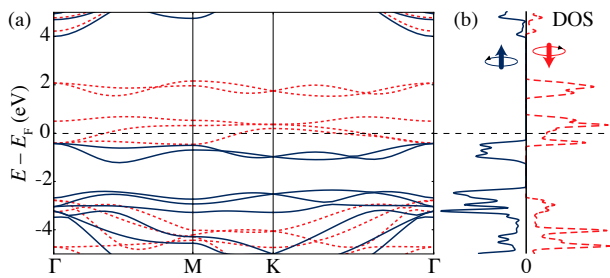


FIG. 7: (Color online) (a) Half-metallic band structure and (b) spin-polarized density of states for 2D FeCl<sub>2</sub>. The minority spin state is metallic (dashed red) and the majority state (solid blue) has a band gap of 4.4 eV.

and R.G.H. were supported under grants DMR-1542776 and PHY-1549132, the Center for Bright Beams. All calculations were performed using the HiPerGator supercomputer at the University of Florida's High Performance Computing Center.

- [1] P. Joensen, R. Frindt, and S. R. Morrison, *Mater. Res. Bull.* **21**, 457 (1986).
- [2] Y. Lin, T. V. Williams, and J. W. Connell, *J. Phys. Chem. Lett.* **1**, 277 (2009).
- [3] O. Altuntasoglu, Y. Matsuda, S. Ida, and Y. Matsumoto, *Chem. Mater.* **22**, 3158 (2010).
- [4] J. N. Coleman, M. Lotya, A. O'Neill, S. D. Bergin, P. J. King, U. Khan, K. Young, A. Gaucher, S. De, R. J. Smith, et al., *Science* **331**, 568 (2011).
- [5] Y.-H. Lee, X.-Q. Zhang, W. Zhang, M.-T. Chang, C.-T. Lin, K.-D. Chang, Y.-C. Yu, J. T.-W. Wang, C.-S. Chang, L.-J. Li, et al., *Adv. Mater.* **24**, 2320 (2012).
- [6] C. Cong, J. Shang, X. Wu, B. Cao, N. Peimyoo, C. Qiu, L. Sun, and T. Yu, *Adv. Opt. Mater.* **2**, 131 (2014).
- [7] X. Li, C. W. Magnuson, A. Venugopal, R. M. Tromp, J. B. Hannon, E. M. Vogel, L. Colombo, and R. S. Ruoff, *J. Am. Chem. Soc.* **133**, 2816 (2011).
- [8] A. K. Singh and R. G. Hennig, *Appl. Phys. Lett.* **105**, 042103 (2014).
- [9] M. Naguib, M. Kurtoglu, V. Presser, J. Lu, J. Niu, M. Heon, L. Hultman, Y. Gogotsi, and M. W. Barsoum, *Advanced Materials* **23**, 4248 (2011).
- [10] M. Ashton, K. Mathew, R. G. Hennig, and S. B. Sinnott, *J. Phys. Chem. C* **120**, 3550 (2016).
- [11] T. Björkman, A. Gulans, A. V. Krasheninnikov, and R. M. Nieminen, *Phys. Rev. Lett.* **108**, 235502 (2012).
- [12] S. Lebègue, T. Björkman, M. Klintonberg, R. M. Nieminen, and O. Eriksson, *Phys. Rev. X* **3**, 031002 (2013).
- [13] A. Jain, S. P. Ong, G. Hautier, W. Chen, W. D. Richards, S. Dacek, S. Cholia, D. Gunter, D. Skinner, G. Ceder, et al., *APL Mater.* **1**, 011002 (2013).
- [14] B. Cordero, V. Gómez, A. E. Platero-Prats, M. Revés, J. Echeverría, E. Cremades, F. Barragán, and S. Alvarez, *Dalton Transactions* pp. 2832–2838 (2008).
- [15] A. K. Singh and R. G. Hennig, *Appl. Phys. Lett.* **105**, 042103 (2014).
- [16] B. C. Revard, W. W. Tipton, A. Yesypenko, and R. G. Hennig, *Phys. Rev. B* **93**, 054117 (2016).
- [17] K.-A. N. Duerloo, M. T. Ong, and E. J. Reed, *J. Phys. Chem. Lett.* **3**, 2871 (2012).
- [18] H. L. Zhuang, M. D. Johannes, M. N. Blonsky, and R. G. Hennig, *Appl. Phys. Lett.* **104**, 022116 (2014).
- [19] W. Wu, L. Wang, Y. Li, F. Zhang, L. Lin, S. Niu, D. Chenet, X. Zhang, Y. Hao, T. F. Heinz, et al., *Nature* **514**, 470 (2014).
- [20] M. N. Blonsky, H. L. Zhuang, A. K. Singh, and R. G. Hennig, *ACS Nano* **9**, 9885 (2015).
- [21] R. Fei, W. Li, J. Li, and L. Yang, *Appl. Phys. Lett.* **107**, 173104 (2015).
- [22] S. Picozzi, *Front. Phys.* **2**, 10 (2014).
- [23] H. L. Zhuang, V. R. Cooper, H. Xu, P. Ganesh, R. G. Hennig, and P. R. C. Kent, *Phys. Rev. B* **92**, 115302 (2015).
- [24] See Supplemental Material at [URL will be inserted by publisher] for top and side views of the 2D structures.
- [25] G. Kresse and J. Hafner, *Phys. Rev. B* **47**, 558 (1993).
- [26] G. Kresse and J. Hafner, *Phys. Rev. B* **49**, 14251 (1994).
- [27] G. Kresse and J. Furthmüller, *Comput. Mater. Sci.* **6**, 15 (1996).
- [28] G. Kresse and J. Furthmüller, *Phys. Rev. B* **54**, 11169 (1996).
- [29] M. Dion, H. Rydberg, E. Schröder, D. C. Langreth, and B. I. Lundqvist, *Phys. Rev. Lett.* **92**, 246401 (2004).
- [30] G. Román-Pérez and J. M. Soler, *Phys. Rev. Lett.* **103**, 096102 (2009).
- [31] J. Klimeš, D. R. Bowler, and A. Michaelides, *J. Phys. Condens. Matter* **22**, 022201 (2009).
- [32] J. Klimeš, D. R. Bowler, and A. Michaelides, *Phys. Rev. B* **83**, 195131 (2011).
- [33] L. Li, Z. Chen, Y. Hu, X. Wang, T. Zhang, W. Chen, and Q. Wang, *J. Am. Chem. Soc.* **135**, 1213 (2013).
- [34] X.-H. Ma, K.-H. Cho, and Y.-M. Sung, *CrystEngComm* **16**, 5080 (2014).
- [35] A. K. Singh, K. Mathew, H. L. Zhuang, and R. G. Hennig, *J. Phys. Chem. Lett.* **6**, 1087 (2015).
- [36] K. S. Novoselov, A. K. Geim, S. Morozov, D. Jiang, Y. Zhang, S. Dubonos, I. Grigorieva, and A. Firsov, *Science* **306**, 666 (2004).
- [37] H. Liu, A. T. Neal, Z. Zhu, Z. Luo, X. Xu, D. Tománek, and P. D. Ye, *ACS Nano* **8**, 4033 (2014).
- [38] S. Zhang, Z. Yan, Y. Li, Z. Chen, and H. Zeng, *Angew. Chem. Int. Ed.* **54**, 3112 (2015).
- [39] P. Ares, F. Aguilar-Galindo, D. Rodríguez-San-Miguel, D. A. Aldave, S. Díaz-Tendero, M. Alcamí, F. Martín, J. Gómez-Herrero, and F. Zamora, *Adv. Mater.* (2016).
- [40] P. Vogt, P. De Padova, C. Quaresima, J. Avila, E. Frantzeskakis, M. C. Asensio, A. Resta, B. Ealet, and G. Le Lay, *Phys. Rev. Lett.* **108**, 155501 (2012).
- [41] H. L. Zhuang and R. G. Hennig, *Appl. Phys. Lett.* **101**, 153109 (2012).
- [42] A. K. Singh, H. L. Zhuang, and R. G. Hennig, *Phys. Rev. B* **89**, 245431 (2014).
- [43] A. K. Singh and R. G. Hennig, *Appl. Phys. Lett.* **105**, 051604 (2014).
- [44] R. A. de Groot, F. M. Mueller, P. G. van Engen, and K. H. J. Buschow, *Phys. Rev. Lett.* **50**, 2024 (1983).
- [45] J.-H. Park, E. Vescovo, H.-J. Kim, C. Kwon, R. Ramesh, and T. Venkatesan, *Nature* **392**, 794 (1998).
- [46] C. M. Fang, G. A. De Wijs, and R. A. De Groot, *J. Appl. Phys.* **91**, 8340 (2002).
- [47] M. N. Baibich, J. M. Broto, A. Fert, F. N. Van Dau,

- F. Petroff, P. Etienne, G. Creuzet, A. Friederich, and J. Chazelas, Phys. Rev. Lett. **61**, 2472 (1988).
- [48] B. Dieny, V. S. Speriosu, S. Metin, S. S. P. Parkin, B. A. Gurney, P. Baumgart, and D. R. Wilhoit, J. Appl. Phys. **69**, 4774 (1991).
- [49] E. W. Hill, A. K. Geim, K. Novoselov, F. Schedin, and P. Blake, IEEE Trans. Magn. **42**, 2694 (2006).
- [50] M. Eschrig, J. Kopu, J. C. Cuevas, and G. Schön, Phys. Rev. Lett. **90**, 137003 (2003).

# Supplementary Information: Topology-Scaling Identification of Layered Solids and Stable Exfoliated 2D Materials

Michael Ashton,<sup>1</sup> Joshua Paul,<sup>1</sup> Susan B. Sinnott,<sup>2</sup> and Richard G. Hennig<sup>1</sup>

<sup>1</sup> Department of Materials Science and Engineering,  
University of Florida, Gainesville, FL 32611-6400

<sup>2</sup> Department of Materials Science and Engineering,  
The Pennsylvania State University, University Park, PA 16801-7003

(Dated: March 6, 2024)

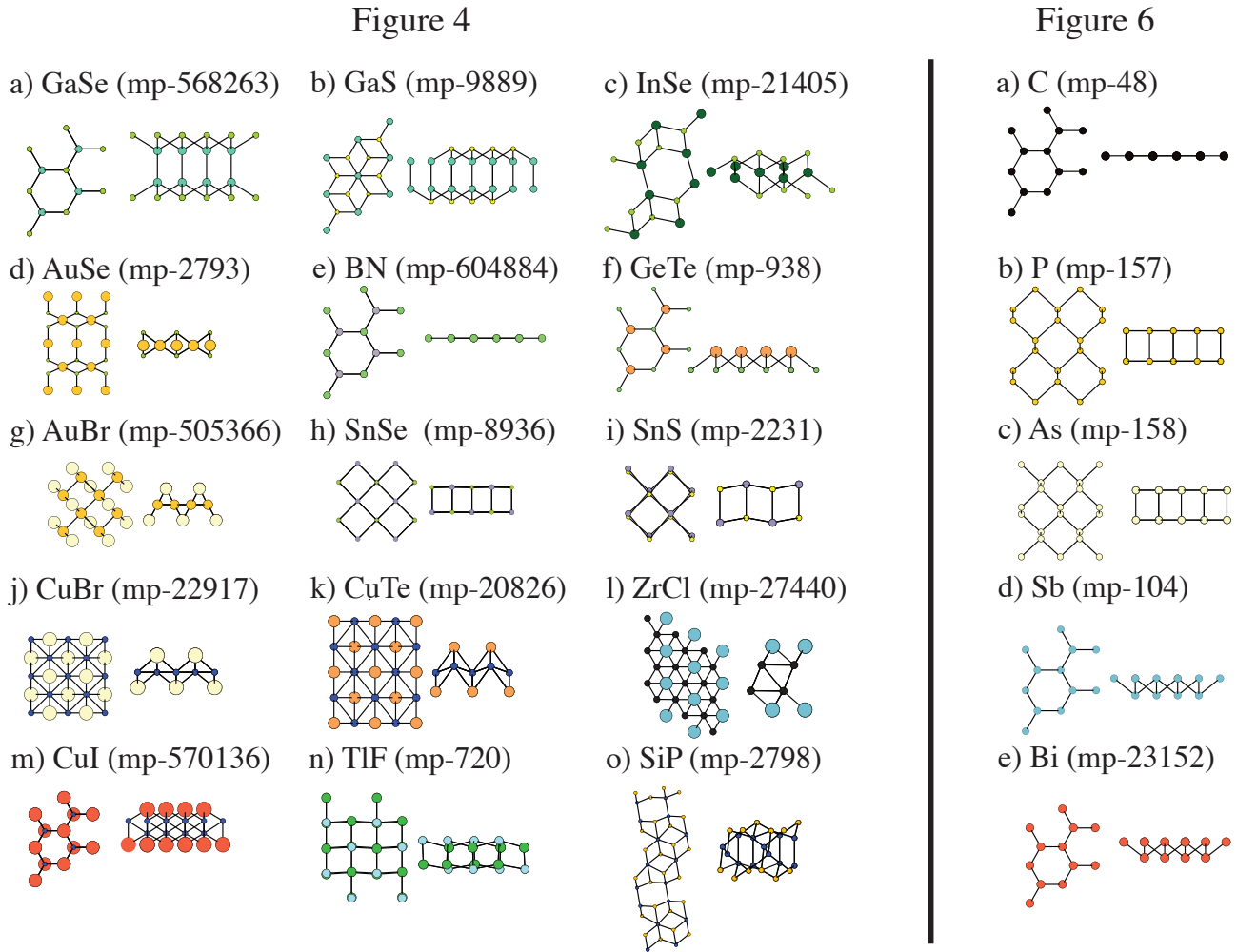


FIG. S1: (Color online) Top (left, for each material) and alternate side (right) views of the crystal structures shown in Figures 4 and 6 from the text. For the 1:1 compounds in Figure 4, the coordination numbers are largely controlled by the octet rule indicating covalent bonding. In structures 4(a) and 4(b), the Ga dimers perpendicular to the 2D layer are bonded to six chalcogen atoms that are either in an eclipsed or staggered configuration. Structure 4(e) is a planar honeycomb structure with three-fold coordinated atoms, a structure shared by graphene in Figure 6(a). Structure 4(f) presents a buckled honeycomb, where the A and B atoms are slightly displaced perpendicular to the plane of the 2D material. This buckled structure is shared by unary materials antimonene and bismene in Figures 6(d) and 6(e). Structures 4(j) and 4(k) are square and rectangular structures, where the halogen and chalcogen atoms are displaced alternately above and below the plane of metal atoms. In structures 4(h) and 4(i), the metal and chalcogen or halide atoms form distorted NaCl(100) structures consisting of two square checkerboard layers with varying small distortions. These structures are quite similar to those of phosphorene and arsenene (6(b) and 6(c)), except that in the unary materials the only distortions from the perfect NaCl(100) are in-plane.